Available online at www.sciencedirect.com

SciVerse ScienceDirect

Ceramics International 39 (2013) 3577–3583

CERAMICS INTERNATIONAL

www.elsevier.com/locate/ceramint

A new $Pb(Lu_{1/2}Nb_{1/2})O_3$–$PbZrO_3$–$PbTiO_3$ ternary solid solution with morphotropic region and high Curie temperature

Tao Li, Xiuzhi Li, Zujian Wang, Ying Liu, Chao He, Liaodong Ai, Tao Chu, Dongfang Pang, Xifa Long*

Key Laboratory of Optoelectronic Materials Chemistry and Physics, Fujian Institute of Research on the Structure of Matter, Chinese Academy of Sciences, Fujian, Fuzhou 350002, China

Received 1 September 2012; received in revised form 10 October 2012; accepted 10 October 2012
Available online 17 October 2012

Abstract

A ceramic ternary system of $(1-x-y)Pb(Lu_{1/2}Nb_{1/2})O_3$–$xPbZrO_3$–$yPbTiO_3$ (PLuN–PZ–PT) has been prepared by two-step synthetic process and characterized by X-ray powder diffraction and electric measurements. A morphotropic phase boundary (MPB) region has been delimited in the ternary system at room temperature. With the PLuN content increasing, the morphotropic phase boundary region becomes broad as well as the dielectric peak. The best comprehensive piezoelectric properties were achieved at MPB composition 0.42PLuN–0.1PZ–0.48PT, with the piezoelectric coefficients d_{33}, the Curie temperature T_c, the planar electromechanical coupling factor K_p, and the remnant polarizations P_r being 367 pC/N, 360 °C, 68% and 35 μC/cm^2, respectively. The results indicate that the PLuN–PZ–PT ternary ferroelectric material may be a promising candidate for high-power electromechanical transducers that can operate in a large temperature range.

Keywords: A. Solid state reaction; C. Piezoelectric properties; C. Ferroelectric properties; D. Perovskite

1. Introduction

Perovskite ferroelectric materials have been extensively studied for actuators, multilayer ceramic capacitors and electromechanical transducers, because of the high dielectric and piezoelectric properties[1–3]. Specifically, the morphotropic phase boundary (MPB) compositions exhibit anomalously high dielectric and piezoelectric properties as a result of enhanced polarizability arising from the coupling between two equivalent energy states, i.e., the tetragonal and rhombohedral phases, allowing optimum domain reorientation during poling [4]. As typical representatives, the piezoelectric and electromechanical properties of $(1-x)Pb(Mg_{1/3}Nb_{2/3})O_3-xPbTiO_3$(PMN–PT) and $(1-x)Pb(Zn_{1/3}Nb_{2/3})O_3-xPbTiO_3$ (PZN–PT) single crystals near MPBs are up to $d_{33}>1500$ pC/N and $k_{33}>0.9$, respectively [5,6].

The usage temperature range, however, is limited by their relatively low ferroelectric–ferroelectric phase transition T_{R-T} (<100 °C), which occurs at significantly lower temperatures than their respective Curie temperature. Furthermore, much attention has been focused on new systems with relatively high T_c and high piezoelectricity near MPBs, such as binary systems of $Pb(Yb_{1/2}Nb_{1/2})O_3$–$PbTiO_3$ (PYN–PT), $BiScO_3$–$PbTiO_3$ (BS–PT), $Pb(In_{1/2}Nb_{1/2})O_3$–$PbTiO_3$ (PIN–PT), etc. [7–9] and ternary systems of $Pb(In_{1/2}Nb_{1/2})O_3$–$Pb(Mg_{1/3}Nb_{2/3})O_3$–$PbTiO_3$ (PIN–PMN–PT), $Pb(Mg_{1/3}Nb_{2/3})O_3$–$Pb(Ni_{1/3}Nb_{2/3})O_3$–$PbTiO_3$ (PMN–PNN–PT), $Pb(Sc_{1/2}Nb_{1/2})O_3$–$Pb(Mg_{1/3}Nb_{2/3})O_3$–$PbTiO_3$ (PSN–PMN–PT), $Pb(Yb_{1/2}Nb_{1/2})O_3$–$Pb(Mg_{1/3}Nb_{2/3})O_3$–$PbTiO_3$ (PYN–PMN–PT) single crystals or ceramics, etc. [10–13].

Specifically, the morphotropic phase boundary (MPB) was observed in PZTs, which displayed excellent piezoelectricity and high T_c ($\sim$370 °C) near the morphotropic phase boundary (MPB) ($x\sim0.47$)[14]. In view of above, numerous studies on PZT-based ternary solid solutions, such as $Pb(Yb_{1/2}Nb_{1/2})O_3$–$PbZrO_3$–$PbTiO_3$ (PYN–PZ–PT) [15], $Pb(Mg_{1/3}Nb_{2/3})O_3$–$PbZrO_3$–$PbTiO_3$ (PMN–PZ–PT) [16] and $Pb(Ni_{1/2}Nb_{1/2})$

*Corresponding author.
Tel.: +86 591 83710369; fax: +86 591 83704907.
E-mail address: lxf@fjirsm.ac.cn (X. Long).

0272-8842/$ - see front matter © 2012 Elsevier Ltd and Techna Group S.r.l. All rights reserved.
http://dx.doi.org/10.1016/j.ceramint.2012.10.184

O_3–$PbZrO_3$–$PbTiO_3$ (PNN–PZ–PT) [17] have been carried out and their MPB compositions were reported to exhibit promising dielectric and piezoelectric properties.

Compositionally ordered $Pb(Lu_{1/2}Nb_{1/2})O_3$ (PLuN) is antiferroelectric with a pseudo-monoclinic perovskite structure and has an antiferroelectric–paraelectric phase transition T_m at 258 °C[18]. It forms a solid solution with $PbTiO_3$ (PT), $(1-x)Pb(Lu_{1/2}Nb_{1/2})O_3-xPbTiO_3$ (PLuN–PT), with a morphotropic phase boundary at $x=0.38$–0.49. The T_c for the MPB composition of this system is up to ~350 °C[18]. To date, however, limited research has been carried out to investigate the PLuN-based binary or ternary systems. In this work, the $(1-x-y)$PLuN–xPZ–yPT ternary system as a function of PT and PZ contents was synthesized; the phase structure, dielectric, ferroelectric and piezoelectric properties were investigated systematically.

2. Experimental procedure

The PLuN–PZ–PT ternary ceramics with the compositions of $(1-x)Pb((Lu_{1/2}Nb_{1/2})_{1-y}Ti_y)O_3-xPbZrO_3$ ($y=0.42-0.50$, $x=0.10$, 0.25, 0.40) were prepared using the two-step precursor method. All the compositions were selected at the proximity of the straight line connecting the two MPBs in binary system PLuN–PT and PZT[14,18]. Raw materials, Lu_2O_3 and Nb_2O_5, were used to synthesize precursor of $LuNbO_4$ at 1150 °C for 1.5 h. Then PbO, TiO_2, ZrO_2, $LuNbO_4$ powders were mixed according to the desired compositions with excess 3 mol% PbO in order to compensate volatilization and wet-milled in alcohol for 24 h. The dried mixed powders were calcined at 800 °C for 6 h to synthesize the compound and then grounded in a mortar for 1.5 h with 5% polyvinyl alcohol binder. The powders were granulated and pressed into pellets. Following binder burnout at 500 °C, the pellets were sintered in a sealed Al_2O_3 crucible at 1050–1150 °C.

The phase structure of the sintered samples was determined by X-ray powder diffraction (Rigaku, Japan) equipped with Cu Kα radiation and a graphite monochromator. The microstructure analyses were undertaken by scanning electron microscopy (SEM: JEOLModel JSM6700F). For electrical tests, sintered samples were polished and coated with silver paste as electrodes. Following this, the samples were poled in silicon oil at 250 °C and electric field of 30 kV/cm. Dielectric measurements were carried out using a computer-controlled Alpha-A broadband dielectric/impedance spectrometer (Novocontrol GmbH), with an AC signal of 1.0 V (peak-to-peak). Polarization hysteresis loops were determined using an aix-ACCT TF2000 analyzer (at $f=2$ Hz) at room temperature. Piezoelectric coefficient was measured using a quasi-static d_{33} meter (Institute of Acoustics, Chinese Academy of Sciences, model ZJ-4AN). The planar electromechanical coupling factor K_p was determined from the resonance and antiresonance frequencies, which were measured using an Alpha-A broadband dielectric/impedance spectrometer (Novocontrol GmbH) according to IEEE standards on piezoelectricity [19,20].

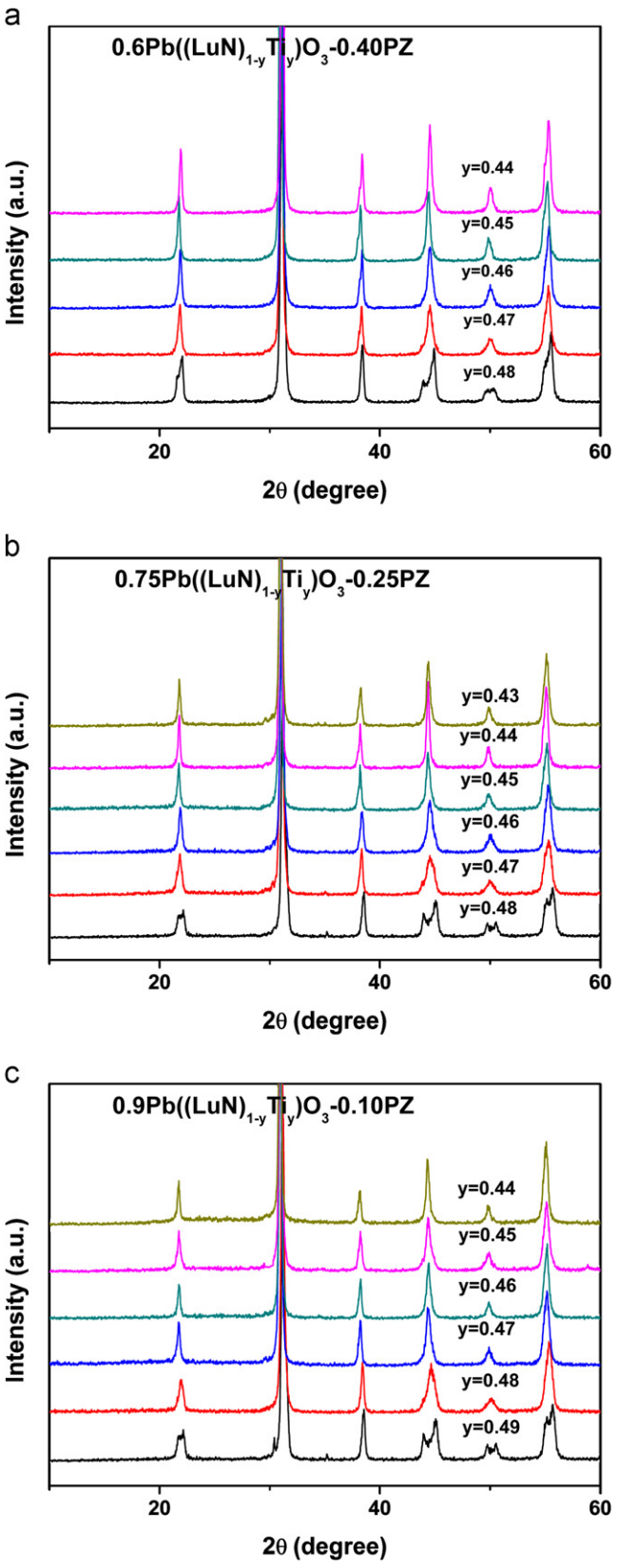

Fig. 1. XRD patterns of $(1-x)Pb((LuN)_{1-y}Ti_y)O_3-xPZ$ ternary system: (a) $x=0.4$, (b) $x=0.25$ and (c) $x=0.1$.

3. Results and discussion

3.1. Structure and phase analysis

The XRD patterns of $(1-x)Pb((Lu_{1/2}Nb_{1/2})_{1-y}Ti_y)O_3-xPbZrO_3$ with various PZ levels are shown in Fig. 1. It can be seen that all the obtained ceramic samples show pure perovskite phase. According to the chemical bonding theory of single crystal growth[21–23], lattice planes correspond to the anisotropic microscopic structure of constituent atoms which finally determine the phase structure of solid state materials. Due to the crystallographic characteristics of perovskite[24,25], the XRD profiles of (200) reflections for the compound with perovskite structure show only a single peak R(200) in the rhombohedral symmetry because all the planes of (200) share the same lattice parameters, however, in the tetragonal symmetry the (200) reflections should be split into two peaks of T(200)/(020) and *T*(002) profiles (due to $a=b\neq c$), with the intensity of the T(200)/(020) peak being double that of T(002) peak. Therefore, the (200) reflections are usually used to distinguish the tetragonal symmetry, rhombohedral symmetry or their coexistence[26,27]. As shown in Fig. 1(a), those samples with $y\geq 0.48$ show the splitting of the pseudo-cubic (200), indicating a tetragonal symmetry for the solid solution with a high PT content. With the PT content decreasing, the (200)/002) peaks gradually merge into one single peak at $y=0.45$, indicating that the structure transfers gradually from tetragonal to rhombohedral phase, in which a morphotropic region is presented within $y=0.46$–0.47. For $x=0.25$ and 0.10, also a similar phenomenon can be observed (as shown in Fig. 1b and c). Based on above analysis, the morphotropic region of PLuN–PZ–PT ternary system has been established, as shown in Fig. 2. Apparently, the morphotropic region became broadened as the composition shifted to the PLuN–PT side. The area above this MPB curve on PT side is in ferroelectric tetragonal phase, while the lower on PT side is in ferroelectric rhombohedral or antiferroelectric phase. Scanning electron microscopy (SEM) images of the fracture surfaces of $0.64Pb(LuN)_{1-x}Zr_x)O_3$–0.46PT and $0.75Pb((LuN)_{1-y}Ti_y)O_3$–0.25PZ, as a function of PZ or PT contents, are given in Figs. 3 and 4, respectively, showing a mixture of transgranular and intergranular characteristics, with low porosity. The grain size of $0.64Pb((LuN)_{1-x}Zr_x)O_3$–0.46PT was found to decrease slightly with decreasing PZ content, being on the order of ~6 μm for $x=0.40$ and ~2 μm for $x=0.10$, as shown in Fig. 3(a)–(c). It should, however, be noted that the compositions with $y=0.46$ were not well-sintered. Meanwhile, the grain size of $0.75Pb((LuN)_{1-y}Ti_y)O_3$–0.25PZ was found to be insensitive to PT content level, being on the order of ~4 μm, as shown in Fig. 4(a)–(c), but the density and the crystallizing quality improved with decreasing PT content, exhibiting good sintering behavior.

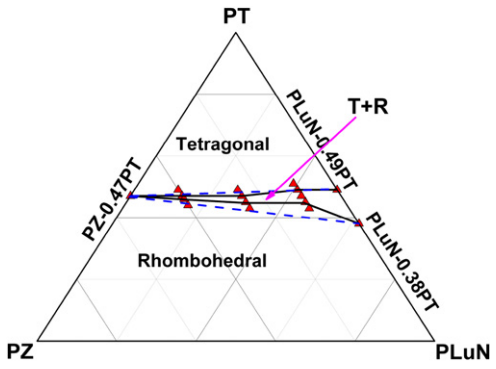

Fig. 2. Phase region of $(1-x)Pb((LuN)_{1-y}Ti_y)O_3-xPZ$ ternary system at room temperature, presenting a morphotropic region.

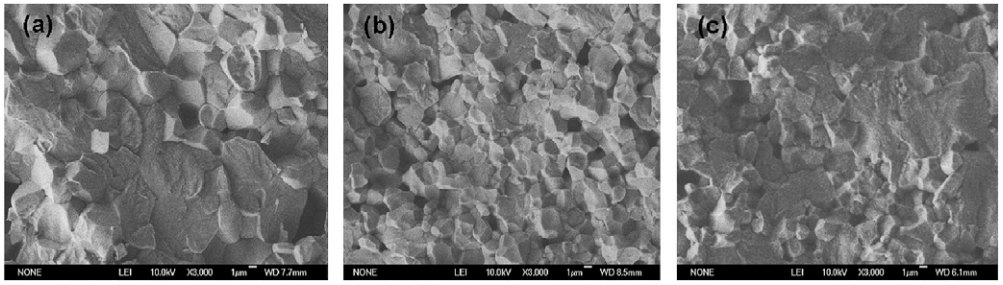

Fig. 3. SEM micrographs of the fracture surface of $0.64Pb((LuN)_{1-x}Zr_x)O_3$–0.46PT: (a) $x=0.40$, (b) $x=0.25$, and (c) $x=0.10$.

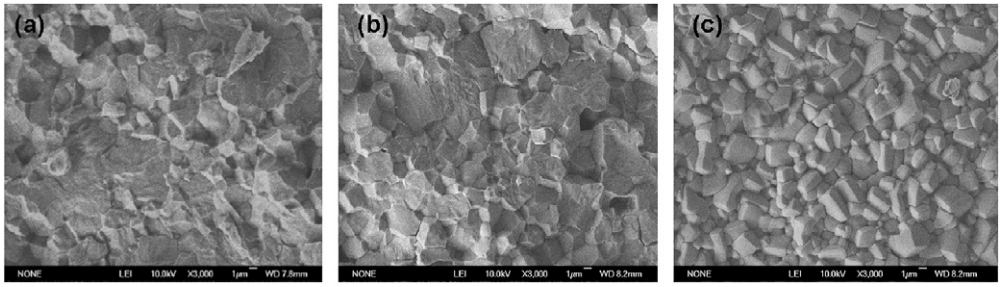

Fig. 4. SEM micrographs of the fracture surface of $0.75Pb((LuN)_{1-y}Ti_y)O_3$–0.25PZ: (a) $y=0.48$, (b) $y=0.45$, and (c) $y=0.43$.

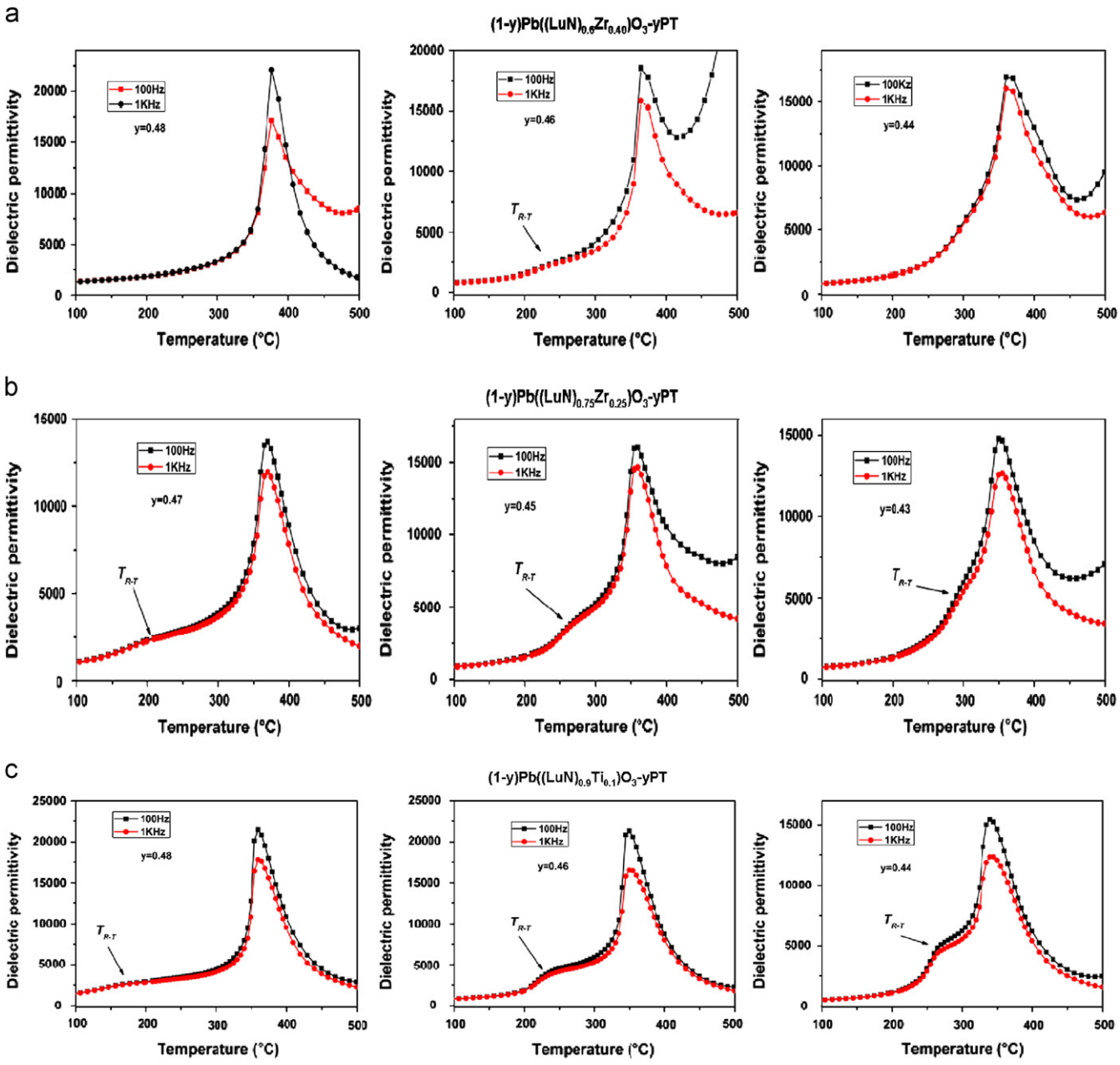

Fig. 5. Temperature dependence of permittivity (ε_r) for $(1-y)$Pb$((\mathrm{LuN})_{1-x}\mathrm{Zr}_x)\mathrm{O}_{3-y}$PT ternary system: (a) $x=0.40$, (b) $x=0.25$, and (c) $x=0.10$.

3.2. Dielectric and piezoelectric properties

(The temperature dependence of dielectric permittivity for $(1-x)$Pb$((\mathrm{LuN})_{1-y}\mathrm{Ti}_y)\mathrm{O}_3-x$PZ is shown in Fig. 5, with corresponding Curie temperature T_c as a function of PT content being given in Fig. 6. It was found that with increasing PT content, T_c increased monotonously, being attributed to the high transition temperature of PT end member ~490 °C. In addition, with increasing PLuN content, the ternary solid solution exhibited more relaxor-like characteristics, showing broadened dielectric peaks and diffused dielectric behavior with respect to frequency. Furthermore, the dielectric anomaly prior to T_c temperature for some compositions could be observed, as indicated in Fig. 5, being associated with the rhombohedral to tetragonal phase transition temperature T_{R-T}, as a result of curved MPB [28,29].

The piezoelectric coefficient d_{33} and dielectric properties at room temperature as a function of PT content with different PZ levels are shown in Fig. 7, showing optimum values for ceramics with MPB compositions. The detailed dielectric, piezoelectric, and electromechanical properties of the studied $(1-x)$Pb$((\mathrm{LuN})_{1-y}\mathrm{Ti}_y)\mathrm{O}_3$-$x$PZ are summarized in Table 1. The optimum properties were achieved in the MPB composition 0.9Pb$((\mathrm{LuN})_{0.52}\mathrm{Ti}_{0.48})\mathrm{O}_3$–0.1PZ ($x=0.10/y=0.48$), with the piezoelectric coefficients d_{33}, the dielectric permittivity ε_r the Curie temperature T_c, the planar electromechanical coupling factor K_p, and the remnant polarizations P_r being on the order of 367 pC/N, 1015, 360 °C, 68% and 35 μC/cm^2,

respectively. It is consistent with the polarization rotation theory of Fu and Cohen due to enhanced polarizability arising from coupling between tetragonal and rhombohedral phase [30].

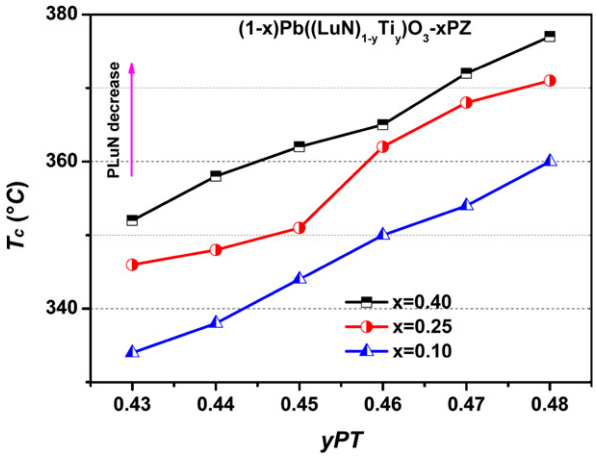

Fig. 6. Curie temperature T_c as a function of PT content for $(1-x)$Pb$((LuN)_{1-y}Ti_y)O_3-x$PZ ternary system.

3.3. Ferroelectric properties

The electric-field-induced bipolar polarization hysteresis loops for $(1-x)$Pb$((LuN)_{1-y}Ti_y)O_3$–xPZ with various PT and PZ levels are shown in Fig. 8, from which remnant polarization P_r and the coercive field E_c as a function of PT content can be obtained, as given in Fig. 9. Remnant polarization P_r was found to increase significantly with increasing PLuN content, reaching peak values for MPB compositions, and then decreasing for compositions with rhombohedral phase, where the maximum value of 39.5 μC/cm^2 was obtained for the MPB composition 0.9Pb$((LuN)_{0.54}Ti_{0.46})O_3$–0.1PZ ($x=0.10/y=0.46$). Due to the coexistence of ferroelectric rhombohedral and tetragonal phases in the MPB region, the highest P_r value is expected owing to the summation of the possible crystallographic orientations, with eight $<111>$ spontaneous polarization directions in a rhombohedral phase and six $<001>$ directions in a tetragonal phase [31]. Meanwhile, E_c was found to increase with increasing PT content, indicating that the domain switching becomes harder with higher PT level, attributed to the decrease of the tetragonal phase.

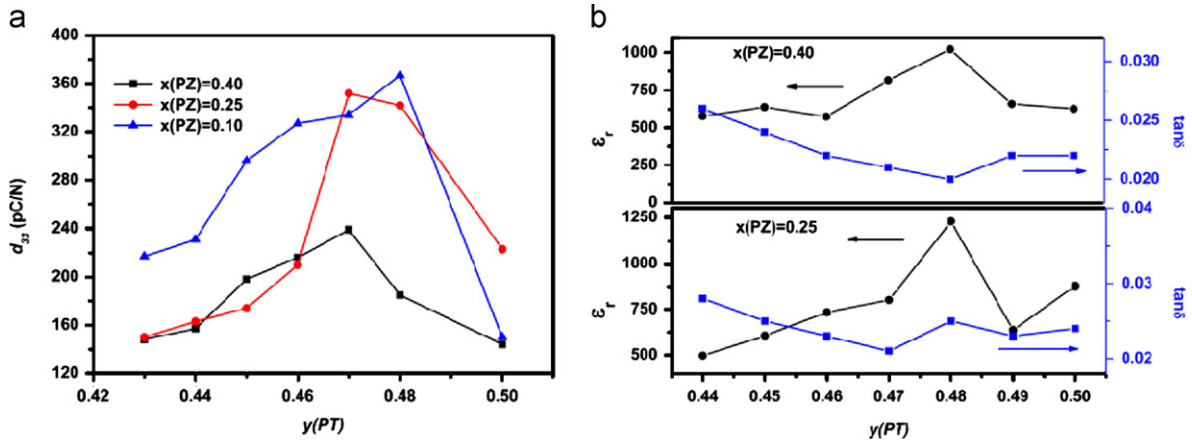

Fig. 7. (a) Piezoelectric coefficient d_{33} and (b) dielectric constant (ε_r) and loss tangent (tan δ) at room temperature and 1 kHz as a function of PT content for $(1-x)$Pb$((LuN)_{1-y}Ti_y)O_3-x$PZ ternary system.

Table 1
Dielectric, piezoelectric, and ferroelectric properties of several selected $(1-x)$Pb$((LuN)_{1-y}Ti_y)O_3-x$PZ ternary ceramics.

Compositions	T_C (°C)	T_{rt} (°C)	ε_r	tan δ	d_{33} (pC/N)	K_p (%)	E_c (kV/cm)	P_r (μC/cm^2)
10PLuN–40PZ–50PT	380	—	876	0.023	144	–	12.98	5.15
12PLuN–40PZ–48PT	377	—	1079	0.020	185	–	13.54	18.55
13PLuN–40PZ–47PT	372	—	1117	0.021	239	43	12.73	19.4
14PLuN–40PZ–46PT	365	235	941	0.023	206	31	11.62	22.9
15PLuN–40PZ–45PT	365	272	836	0.024	198	–	11.43	14.9
27PLuN–25PZ–48PT	371	—	1308	0.021	342	48	14.81	27.6
28PLuN–25PZ–47PT	368	200	965	0.022	352	56	13.66	26.18
29PLuN–25PZ–46PT	362	232	790	0.023	210	–	10.72	23.8
30PLuN–25PZ–45PT	351	264	652	0.025	174	–	10.3	22.6
32PLuN–25PZ–43PT	346	291	538	0.028	150	–	8.9	21.2
42PLuN–10PZ–48PT	360	177	1015	0.017	367	68	16.97	34.9
43PLuN–10PZ–47PT	355	204	978	0.020	334	54	15.9	29.5
44PLuN–10PZ–46PT	350	232	946	0.026	327	52	15.54	37.5
45PLuN–10PZ–45PT	344	243	902	0.019	296	–	15.02	35.3
46PLuN–10PZ–44PT	338	260	821	0.018	217	–	14.7	33.6
47PLuN–10PZ–43PT	331	—	804	0.020	203	–	13.2	29.6

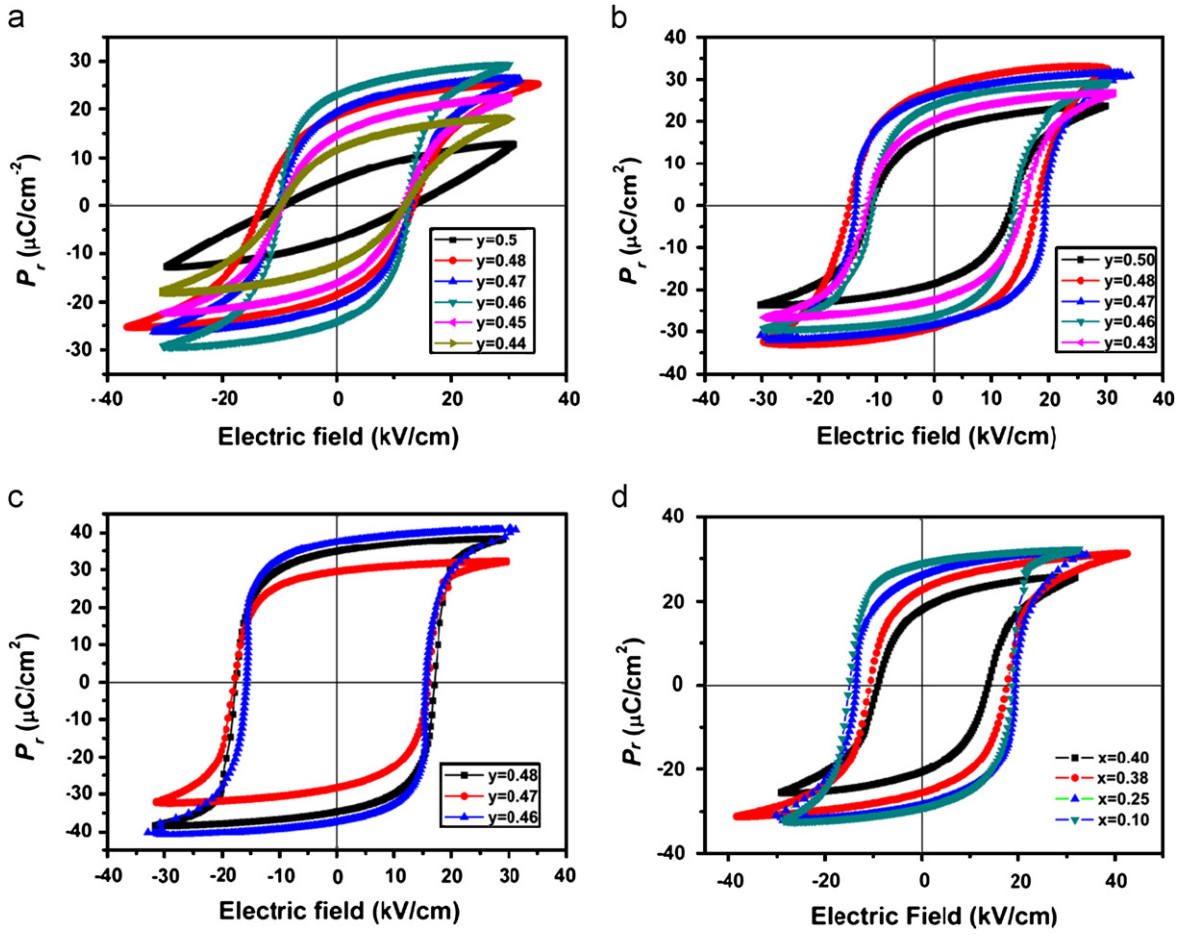

Fig. 8. Bipolar polarization hysteresis loops for $(1-x)Pb((LuN)_{1-y}Ti_y)O_3-xPZ$ ternary system: (a) $x=0.4$, (b) $x=0.25$, (c) $x=0.1$, and (d) $y=0.47$.

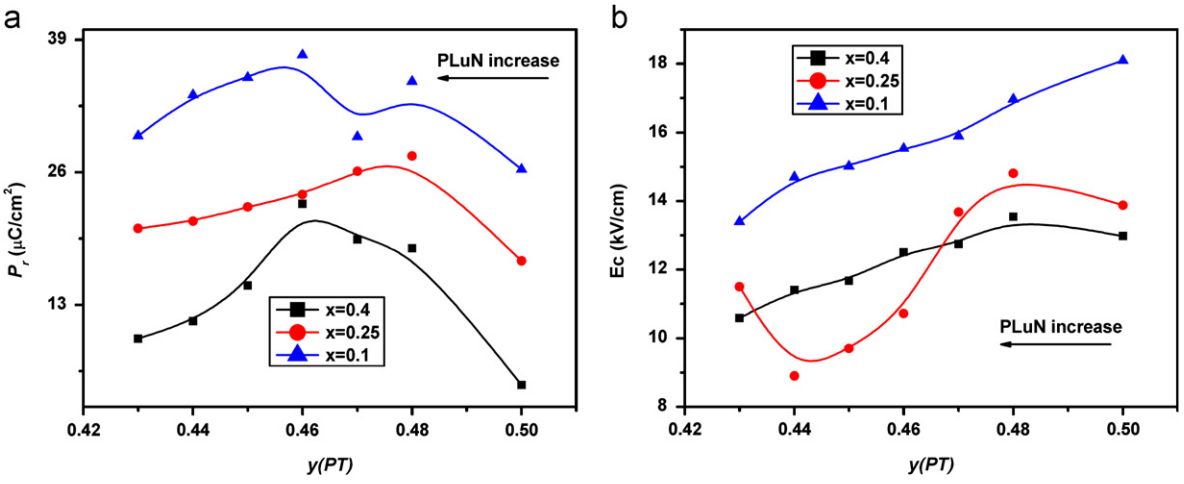

Fig. 9. Remnant polarization P_r (a) and coercive field E_c (b) as a function of PT content for $(1-x)Pb((LuN)_{1-y}Ti_y)O_3-xPZ$ ternary system.

4. Conclusions

In conclusion, the $(1-x)Pb((Lu_{1/2}Nb_{1/2})_{1-y}Ti_y)O_3$–$xPbZrO_3$ ternary system with compositions near MPB was prepared using two-step synthetic process. The phase structure, dielectric, piezoelectric, and ferroelectric properties were investigated systematically. The MPB region in the phase diagram for the ternary system was delimited. As compositions shift to the PLuN–PT side, the morphotropic phase boundary region became broader. Meanwhile, the dielectric behavior exhibited the relaxor-like characteristics. The optimum properties were achieved at the MPB composition 0.42PLuN–0.10PZ–0.48PT, with the piezoelectric coefficients d_{33} of 367 pC/N, the Curie temperature T_C of 360 °C, the electromechanical coupling factor K_p of 68% and the remnant polarizations P_r of 34.9 μC/cm^2, exhibiting

potential usage for high-powder electromechanical transducers that can be operated in a large temperature range.

Acknowledgments

This work was supported by a grant from the National High Technology Research and Development Program of China (863 Program; No. 2011AA030208) and the National Natural Science Foundation of China under Grant no.91122020.

References

[1] S.-E. Park, T.R. Shrout, Ultrahigh strain and piezoelectric behavior in relaxor based ferroelectric single crystals, Journal of Applied Physics 82 (1997) 1804–1811.
[2] S.-E. Park, T.R. Shrout, Relaxor based ferroelectric single crystals for electro-mechanical actuators, Materials Research Innovations 1 (1997) 20–25.
[3] T.R. Shrout, R. Eitel, S.J. Zhang, C. Randall, E. Alberta, P. Rehrig, Recent developments in transition temperature (T_c) perovskite crystals, Ultrasonics 1 (2003) 774–777.
[4] S.J. Zhang, R. Xia, L. Lebrun, D. Anderson, T.R. Shrout, Piezoelectric materials for high power, high temperature applications, Materials Letters 59 (2005) 3471–3475.
[5] S.-E. Park, T.R. Shrout, Ultrahigh strain and piezoelectric behavior in relaxor based ferroelectric single crystals, Journal of Applied Physics 82 (1997) 1804–1811.
[6] S.-E. Park, T.R. Shrout, Relaxor based ferroelectric single crystals for electro-mechanical actuators, Materials Research Innovations 1 (1997) 20–25.
[7] S.J. Zhang, S. Rhee, C.A. Randall, T.R. Shrout, Dielectric and piezoelectric properties of high Curie temperature single crystals in the $Pb(Yb_{1/2}Nb_{1/2})O_3-xPbTiO_3$ solid solution series, Japanese Journal of Applied Physics 41 (2002) 722.
[8] R.E. Eitel, C.A. Randall, T.R. Shrout, S.-E. Park, Preparation and characterization of high temperature perovskite ferroelectrics in the solid-solution $(1-x)BiScO_3$–$xPbTiO_3$, Japanese Journal of Applied Physics 41 (2002) 2099–2104.
[9] N. Yasuda, H. Ohwa, M. Kume, Y. Yamashita, Piezoelectric properties of a high curie temperature $Pb(In_{1/2}Nb_{1/2})O_3$–$PbTiO_3$ binary system single crystal near a morphotropic phase boundary, Japanese Journal of Applied Physics 39 (2000) 66–69.
[10] Y. Hosona, Y. Yamashita, H. Sakamoto, N. Ichinose, Dielectric and piezoelectric properties of $Pb(In_{1/2}Nb_{1/2})O_3$–$Pb(Mg_{1/3}Nb_{2/3})O_3$–$PbTiO_3$ ternary ceramic materials near the morphotropic phase boundary, Japanese Journal of Applied Physics 42 (2003) 535–538.
[11] C. Lei, K. Chen, X. Zhang, Structure and dielectric relaxation behavior near the MPB for $Pb(Ni_{1/3}Nb_{2/3})O_3$–$Pb(Mg_{1/3}Nb_{2/3})O_3$–$PbTiO_3$ ferroelectric ceramics 111 (2004) 107–112.
[12] Y. Guo, H. Xu, H. Luo, G. Xu, Z. Yin, Growth and electrical properties of $Pb(Sc_{1/2}Nb_{1/2})O_3$–$Pb(Mg_{1/3}Nb_{2/3})O_3$–$PbTiO_3$ ternary single crystals by a modified Bridgman technique 226 (2001) 111–116.
[13] C. He, X. Li, Z Wang, X. Long, S. Mao, Z.-G. Ye, Preparation and characterization of new $Pb(Yb_{1/2}Nb_{1/2})O_3$–$Pb(Mg_{1/3}Nb_{2/3})O_3$–$PbTiO_3$ ternary piezo-/ferroelectric crystals, Chemistry of Materials 22 (2010) 5588–5592.
[14] B. Jaffe, R.S. Roth, S. Marzullo, Piezoelectric properties of lead zirconate titanate solid-solution ceramics, Journal of Applied Physics 25 (1954) 809–810.
[15] H. Ohuchi, S. Tsukamoto, M. Ishii, H. Hayakawa, Piezoelectric and structural properties of $Pb(Yb_{1/2}Nb_{1/2})O_3$–$PbTiO_3$–$PbZrO_3$ ceramics, Journal of European Ceramic Society 19 (1999) 1191–1195.
[16] H. Ohuchi, K. Nagano, S. Hayakawa, Piezoelectric properties of $Pb(Mg_{1/3}Nb_{2/3})O_3$–$PbTiO_3$–$PbZrO_3$ solid solution ceramics, Journal of the American Ceramic Society 48 (1965) 630–635.
[17] R. Cao, G. Li, J. Zeng, S. Zhao, L. Zheng, Q. Yin, The piezoelectric and dielectric properties of $0.3Pb(Ni_{1/3}Nb_{2/3})O_3-xPbTiO_3$–$(0.7-x)PbZrO_3$ ferroelectric ceramics near the morphotropic phase boundary, Journal of the American Ceramic Society 93 (2010) 737–741.
[18] M. Antonova, L. Shebanovs, M. Livinsh, J.Y. Yamshita, A. Sternberg, I. Shorubalko, A. Spluse, Structure and properties of hot-pressed $Pb(Lu_{1/2}Nb_{1/2})O_3$–$PbTiO_3$ binary system ceramics, Journal of Electroceramics 4 (2000) 179–187.
[19] Standards Committee of the IEEE Ultrasonics, Ferroelectrics and Frequency Control Society, IEEE Standard on Piezoelectricity, American National Standards Institute, New York, 1987.
[20] S.J. Zhang, E.F. Alberta, R.E. Eitel, C.A. Randall, T.R. Shrout, Elastic, piezoelectric, and dielectric characterization of modified $BiScO_3$–$PbTiO_3$ ceramics, IEEE Transactions on Ultrasonics, Ferroelectrics and Frequency Control 52 (2005) 2131–2139.
[21] C.T. Sun, S.Y. Song, D.F. Xue, H.J. Zhang, Crystallization of oxides as fuctional materials, Functional Materials Letters 5 (2012) 1230002.
[22] X.X. Yan, D.L. Xu, D.F. Xue, SO_4^{2-} ions direct the one-dimensional growth of $5Mg(OH)_2 \ldots MgSO_4 \cdot 2H_2O$, Acta Materialia 55 (2007) 5747–5757.
[23] D.L. Xu, D.F. Xue, Chemical bond analysis of the crystal growth of KDP and ADP, Journal of Crystal Growth 286 (2006) 108–113.
[24] H. Zhang, N. Li, K. Li, D.F. Xue, Structural stability and formability of ABO(3)-type perovskite compounds, Acta Crystallographica Section B 63 (2007) 812–818.
[25] Y.M. Zhang, R. Ubic, D.F. Xue, S. Yang, Compounds using artificial neural networks, Materials Focus 1 (2012) 57–64.
[26] J. Yuan, D.W. Wang, H.B. Lin, Q.L. Zhao, D.Q. Zhang, M.S. Cao, Effect of ZnO whisker content on sinterability and fracture behaviour of PZT piezoelectric composites, Journal of Alloys and Compounds 504 (2010) 123–128.
[27] H. Hao, S.J. Zhang, H.X. Liu, T.R. Shrout, Dielectric, piezoelectric, and electromechanical properties of morphotropic phase boundary compositions in the $Pb(Mg_{1/3}Ta_{2/3})O_3$–$PbZrO_3$–$PbTiO_3$ ternary system, Journal of Applied Physics 105 (2009) 024104–024106.
[28] S. Choi, T. Shrout, S. Jang, A. Bhalla, Dielectric and pyroelectric properties in the $Pb(Mg_{1/3}Nb_{2/3})O_3$–$PbTiO_3$ system, Ferroelectrics 100 (1989) 29–38.
[29] D.W. Wang, M.S. Cao, S.J. Zhang, Phase diagram and properties of $Pb(In_{1/2}Nb_{1/2})O_3$–$Pb(Mg_{1/3}Nb_{2/3})O_3$–$PbTiO_3$ polycrystalline ceramics, Journal of the European Ceramic Society 32 (2012) 433–439.
[30] H. Fu, R.E. Cohen, Polarization rotation mechanism for ultrahigh electromechanical response in single crystal piezoelectrics, Nature 403 (2000) 281.
[31] C.A. Randall, N. Kim, J. Kucera, W. Cao, T.R. Shrout, Intrinsic and extrinsic size effects in fine-grained morphotropic-phase-boundary lead zirconate titanate ceramics, Journal of the American Ceramic Society 81 (1998) 677–688.